RSC Advances

ROYAL SOCIETY OF CHEMISTRY

www.rsc.org/advances

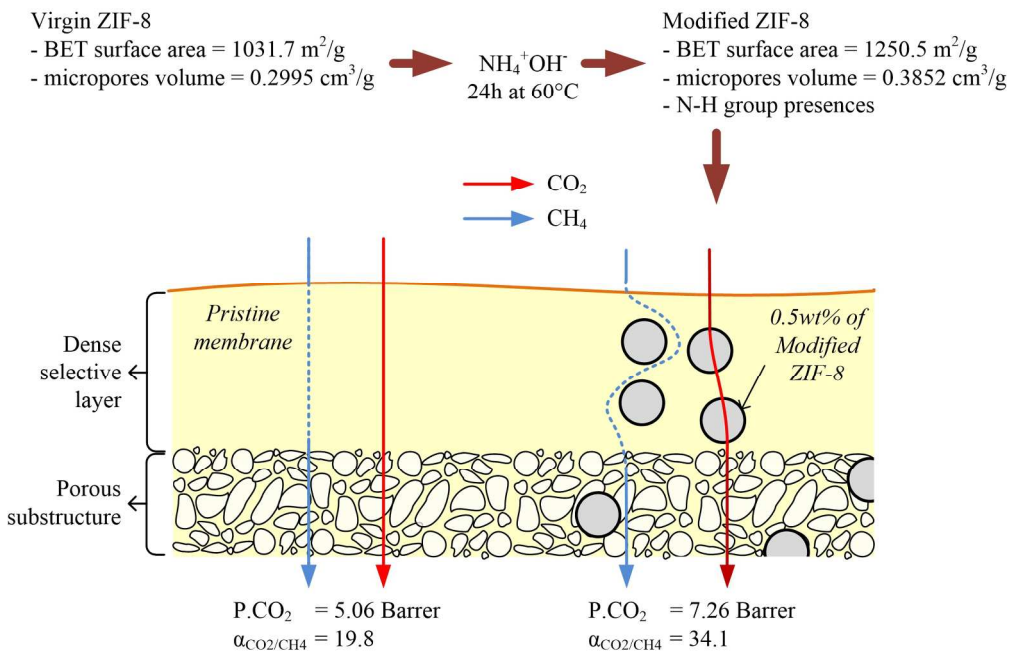

Graphical Abstract Facile ammonia modification introduced N-H group to the ZIF-8 particles while increased its BET surface area and micropores volume. The MMM consist of modified ZIF-8 has provide excellent CO2-selective feature and increase CO2 permeability up to 43% and ideal CO2/CH4 selectivity up to 72% even only 0.5wt% fillers was embodied.
181x117mm (300 x 300 DPI)

Facile modification of ZIF-8 mixed matrix membrane for CO_2/CH_4 separation: synthesis and preparation

Nik Abdul Hadi Md Nordin[a], Surya Murali Racha[a], Takeshi Matsuura[b], Nurasyikin Misdan[a], Nur Aimie Abdullah Sani[a], Ahmad Fauzi Ismail*[a], & Azeman Mustafa[a]

[a] Advanced Membrane Technology Research Centre (AMTEC), Universiti Teknologi Malaysia, 81310 Skudai, Johor, Malaysia

[b] Industrial Membrane Research Laboratory, Department of Chemical and Biological Engineering, University of Ottawa, Ottawa, Ontario, Canada

* Corresponding author. Tel.: +6075535592; fax: +6075581463.

E-mail address: afauzi@utm.my, fauzi.ismail@gmail.com (A.F. Ismail)

Abstract

Metal organic framework (MOF) possess tunable characteristic that allowed various modifications to be practiced and satisfying specific applications. In this study, zeolitic imidazole framework 8 (ZIF-8) was synthesized and subjected to ammonia modification under different temperature and ammonia solution loading. The presence of N-H group observed after the modification indicates the successful modification of ZIF-8. The modified ZIF-8 showed notable changes with increased phase crystallinity, micropore volume and BET surface area. The unmodified and modified ZIF-8s were then dispersed into polysulfone (PSf) matrix, and the MMMs were prepared via dry/wet phase inversion. No apparent differences in membrane's morphology and thermal stability were noticed between neat PSf membrane and MMMs. The MMMs were further subjected to pure CO_2 and CH_4 gas permeation experiments. CO_2 permeance decreased while CO_2/CH_4 selectivity increased as a result of ZIF-8 modification, due to the decrease in mesopore contribution and the increase in micropore contribution to the gas permeation path. The affinity of N-H group in the modified ZIF-8 to CO_2 also contributed to the increase of CO_2 permeance. For example, when ZIF-8 modified in 25mL ammonia solution at 60°C (Z25c) was dispersed in PSf matrix, the CO_2/CH_4 selectivity increased 72% and CO_2 permeability to 43% compared to the neat PSf membrane.

Keywords: ZIF-8, ammonia modification, PSf/ZIF-8, asymmetric mixed matrix membrane

1. Introduction

The depletion of natural gas resources as well as their worsening quality are great concern nowadays. It was reported that the natural gas usually consists of up to 80% of impurities, depending on geographical factors[1]. Among the impurities in natural gas, CO_2 is considered as the most crucial species that need to be intensively removed. Aside from environmental issues such as the main culprit of climate change, the presence of CO_2 in the process streams would decrease the heating value, increase pipeline corrosion, and consequently lead to increase in operational and maintenance cost. The challenges arise to ensure that the presence of CO_2 in pipeline is below 0.2% based on U.S. pipeline specifications before the product is delivered to customers. Hence, an efficient CO_2 removal system is necessary. The well-developed processes for CO_2 removal such as amine absorption, pressure swing adsorption and cryogenic distillation have been implemented over the years and have demonstrated to be reliable in large scale operation and adaptable for many industries[2, 3]. However, limitations of the conventional processes such as high solvent losses and degradation, unit corrosion, high maintenance, high energy requirement, and refrigerant toxicity[4, 5] have driven for the search of more economical and efficient gas separation system.

Over the years, the attention has been focused on polymeric membrane for natural gas separation. Polymeric membranes are advantageous in terms of versatility in wide-range of CO_2 concentrations, low operating cost, modest energy requirement, and space efficiency compared to the conventional processes[6]. In addition, membrane as a pressure-driven process would be practical for high pressure system in natural gas processing and requires no additional compression units to transport the retantate stream[5]. However, polymeric membranes are bounded by the Robeson trade-off limit between permeability and selectivity, which has hindered its potential application in gas separation[7]. Although new class of polymer such as Thermally Rearrange (TR) polymer and polymer of intrinsic microporosity (PIM) has shown promising candidate for gas separation[8], their development are still under investigation and unlikely to be commercially available for large scale membrane production in the next few years.

Limitations suffered by polymeric membranes have led to research for inorganic membranes as alternatives. Inorganic membranes such as zeolites and carbon membranes offer several advantages over conventional polymeric membranes in terms of mechanical strength, thermal stability and resistance towards a wide range of chemicals. Particularly, inorganic

membranes provide better permeability and selectivity, exceeding Robeson's upperbound suffered by polymeric membranes. Despite its prevalence, fabricating continuous defect free inorganic membranes is a challenge due to their brittle structure. As well, requirement of extensive fabrication energy is one of the obstacles that hinder their diverse applications. Hence, recent membrane development has been focused on mixed matrix membranes (MMM), combination of polymeric membrane as continuous phase with inorganic particle as disperse phase. Incorporated filler into polymer matrix can either improve permeability while maintaining gas pair selectivity[9] or improve gas pair selectivity without expense of permeability[10] or improve both permeability and selectivity[11]. Besides, the two phases compensate each phase's limitations and improved processibility, mechanical strength, thermal and chemical stability also motivate the further research on MMM[12]. Previous studies have shown promising results by utilizing zeolites[10, 13], carbon nanotube (CNT)[14], carbon molecular sieve (CMS)[15], activated carbon[16] and metal organic framework (MOFs)[17] as the disperse phase.

Development of defect-free MMM remains as a challenging task as polymer-filler compatibility is often insufficient to formed homogeneous interface[18]. The polymer-filler incompatibility would provoke filler to repulse the continuous phase and form "sieve-in-cage" morphology, which is responsible for unselective voids. The unselective voids are more preferable for penetrant to permeate across the membrane since it provides negligible mass transport resistance without discriminating penetrants. Hence, selection of the dispersed phase is a crucial factor to develop defect-free MMM. Compared to other classes of fillers, MOFs have shown to have good interaction with polymer matrix through its organic ligands. MOFs are crystalline compounds that consist of metal ions and secondary building unit (SBU) or organic ligands. Besides, large surface area, high micropore volume, various pore sizes, crystallinity and a high metal content has let MOFs emerge as spectacular porous materials for diverse applications[19]. Zeolite Imidazole Framework-8 (ZIF-8), a product between Zn^{2+} with 2-methylimidazole (2-MeIM), is one of the most investigated MOFs. ZIF-8 properties are widely studied to show very good chemical stability against polar and nonpolar solvents[20], reorientation of its structure at high pressure[21] and high mechanical strength[22].

Nonetheless, MOF membrane suffers from low intrinsic CO_2/CH_4 selectivity and therefore it has been mainly studied as adsorption media[23-25]. In case of ZIF-8, it offers intrinsic CO_2/CH_4 selectivity <5, significantly lower than other inorganic membranes such as zeolite T[26]

and carbon membrane[27]. Hence, modifications are necessary to further improve its affinity towards CO_2 before implemented as membrane's filler for CO_2/CH_4 separation. MOF has been known for its tunable properties and ease for modification. Modifications of MOF are practiced to alter its pore structure, pore aperture, surface functional groups, and chemical stability, depending on specific applications[28-31]. Notably, post-synthetic modifications have demonstrated as straightforward modification approach with significant improvement of MOF properties. For example, metal ion doping into MOF to provide open metal sites has significantly improved gas adsorption capacity of MOF. Metal ions such as potassium, sodium and lithium are used to provide additional interaction with quadrupole moment of gases while enhancing molecular sieving through restricted pore size of modified MOF[24, 32]. On the other hand, modifying MOF through ligands also proved to be a convincing approach. Introducing functional groups such as pyridine and amine to the MOF structure would increase its affinity towards quadrupole moment gases such as CO_2 and H_2[23, 33]. For example, Zhang *et al*.[34] has demonstrated that ammonia impregnated ZIF-8 provides additional basic sites within the pores and resultant increased CO_2 uptake up to 50% as compared to virgin ZIF-8 without changes in the crystal integrity. In short, tunability of MOF would significantly improve its properties and its potential as fillers for MMM and would give distinctive factors on gas separations.

Although ammonia-based modifications of ZIF-8 have demonstrated to be an attractive approach to increase affinity towards CO_2, the implementation of the modified particle as dispersed phase in MMM is yet to be investigated. This issue is crucial to be investigated since modifications may result in closed pores, which would significantly deteriorate the MMM performance. Herein, we are to report preparation and characterization of improved CO_2 selective MMM using modified ZIF-8 for CO_2/CH_4 separation. The ammonia modified ZIF-8 particles were prepared under different modification protocols and their properties were stringently studied before being dispersed into polymer matrix. Polysulfone (PSf) was selected as the polymeric phase since it is abundant and cheap material while providing well balanced CO_2 permeability and CO_2/CH_4 selectivity. Asymmetric MMMs were fabricated using dry/wet phase inversion method by incorporation of modified ZIF-8s under different modification protocols. The effect of the ZIF-8 embodiment on overall membrane properties and the CO_2/CH_4separation is evaluated.

2. Experimental

2.1 Materials

Zinc nitrate hexahydrate ($Zn(NO_3)_2.6H_2O$) was purchased from Alfa Aesar. Chemicals such as 2-methylimidazole (2-MeIM), n-hexane, polydimethylsiloxane (PDMS) and triethylamine (TEA) were obtained from Sigma Aldrich. Polysulfone (PSfUdel® P-1700) with density of 1.24 g/cm^3 was procured from Solvay Plastic. Ammonium hydroxide solution (25%), *N,N*-methylpyrrolidone (NMP), tetrahydrofuran (THF) and ethanol were purchased from Merck. All chemicals were used without further purification.

2.2 ZIF-8 Synthesis

ZIF-8 was prepared by following the same procedure as described in our previous work [35] with the ratio of $Zn(NO_3)_2$:2-MeIM:H_2O 1:6:500. Briefly, metal salt solution was prepared by dissolving 2g of $Zn(NO_3)_2.6H_2O$ (6.72 mmol) in 12.11g of deionized water (20% of total deionized water). For ligand solution, 2-MeIM (3.312g, 40.34 mmol) was dissolved into 48.45g of deionized water and subsequently 3.0 mL of TEA was added. The metal salt solution was gently added to the ligand solution, resulting in a cloudy solution mixture. The solution was stirred vigorously for 30 minutes, followed by centrifugation of the reaction product. The obtained product was washed several times with deionized water to remove excess reactants and subsequently dried in an oven at 60°C for 12 hours. The collected powder was ground into fine particles before further dried in an oven at 100°C for minimum of 12 hours to further evacuate the guest molecules in the ZIF-8 pores.

2.3 ZIF-8 modification parameters

Synthesized ZIF-8s were indigenously modified as follows. Firstly, 1.0 g of the prepared ZIF-8 was uniformly dispersed into predetermined volume of ammonium hydroxide solution (**Table 1**) with additional 10 mL deionized water. The suspension was then sonicated for 60 minutes to break the particle bulks before being vigorously stirred for 24 h at specific temperatures. The sample was collected via centrifugation and washed with deionized water (3 times) before being dried in an oven (60°C) overnight. ZIF-8 modification parameters are listed in **Table 1**.

Table 1. ZIF-8 modifications parameters

ZIF-8 samples	Ammonia solution (mL)	Temperature	MMM
Z-0	-	-	M0
Z25a	25	Ice bath (4°C)	M25a
Z25b	25	Room temperature	M25b
Z25c	25	60°C	M25c
Z50a	50	Ice bath (4°C)	M50a
Z50b	50	Room temperature	M50b
Z50c	50	60°C	M50c

2.4 Asymmetric Flat Sheet Membrane Preparation

Asymmetric flat sheet MMM was prepared from the solution that consisted of PSf (25wt%), NMP (60wt%), THF (15wt%) and ZIF-8 (0.5wt% of the total solids unless otherwise stated). ZIF-8 was dispersed into NMP/THF solvent and approximately 10% of polymer was added under stirring for the priming purpose. Remaining polymer was gradually added and the mixture was kept stirred until the solution became homogeneous. The casting dope was then hand-cast using a casting bar to a thickness of 120-190 μm. After standing on the glass plate for approximately 3 min, the cast film together with the glass plate was immersed in a coagulation bath (water at 27 °C) where the membrane was solidified. Then, the membrane was transferred to fresh water and kept there for 1 day to remove the residual solvent completely. Finally, the membrane was solvent-exchanged by immersing progressively in methanol and n-hexane, each for 2 h, before being air-dried for 24 hours in the ambient atmosphere. The pristine PSf membrane was prepared by the same process without adding ZIF-8. The surface of the membrane was then brought into contact with 3wt% PDMS/n-hexane solution for 10 min to seal possible pinholes before they were "cured" at 60°C for 12 hours. Sample abbreviations are listed in **Table 1**.

2.5 Characterization

Attenuated total reflectance Infrared Spectroscopy (ATR-IR) analysis was conducted using Perkin Elmer UATR (Single Reflection Diamond) for Spectrum Two to observe the functional groups of the modified ZIF-8s.

Differential scanning calorimeter (DSC) was used to determine the glass transition temperature (T_g) of the prepared membranes after incorporating the filler into polymer matrix by using Mettler Toledo DSC 822e. The membrane sample was cut into small pieces, weighed and placed into pre-weighed aluminium crucible. Then, the sample was heated from 50 to 400°C at a heating rate of 10°C min^{-1} in the first cycle to remove the thermal history. The sample was cooled from 400 to 30°C at the rate of 10°C min^{-1}. The same heating protocol was repeated in the next heating cycle. T_g of the sample was determined as the midpoint temperature of the transition region in the second heating cycle.

Thermogravimetric analysis (TGA) was used to characterize thermal stability of the prepared samples. TGA records the weight changes of the sample when heated continuously. The sample was heated from 50 to 900°C at the heating rate of 10°C min^{-1} under nitrogen atmosphere with a nitrogen flow rate of 20 mL min^{-1}.

XRD analysis was used to confirm that the phase of ZIF-8 was similar to that reported in the literature and to monitor the changes in ZIF-8 crystallinity after modification. X-Ray Diffraction (XRD) analysis using Siemens D5000 Difractometer is non-destructive analysis to identify the structure of the sample by measuring 2θ angles. The XRD will emit x-rays to the sample and the x-rays are diffracted at different angles and intensities by using CuKα radiation with a wavelength (λ) = 1.54Å at room temperature.

The specific surface area and pore volume of the virgin ZIF-8 and modified ZIF-8 crystals were measured by using Micromeritics gas adsorption analyzer ASAP2010 instrument equipped with commercial software for calculation and analysis. The BET surface area was calculated from the adsorption isotherms using the standard Brunauer–Emmett–Teller (BET) equation. The total pore volume was evaluated by converting the adsorption amount at p/p_0=0.95 to a volume of liquid adsorbate. The mesopores volume was obtained using the BJH plot while micropores volume was obtained using the t-plot method of the Lippens and de Boer to the adsorption data.

Scanning electron microscopy (SEM) was used to observe the membrane structure and morphology. Membrane samples were fractured cryogenically in liquid nitrogen. The samples

were coated with gold before they were imaged and photographed by employing a scanning electron microscope (TM3000, Hitachi) with a potential of 10 kV under magnifications ranging from 1,000 to 20,000.

Transmission electron microscope (TEM) (JEOL, JSM-6701FJEOL 1230) was applied to observe the macrostructures of the ZIF-8. Samples were prepared by dispersing ZIF-8 powder into methanol. A drop of methanol was used for the dispersion of ZIF-8 on carbon-coated copper grids operating at 300 kV.

Gas permeation tests were performed using a constant pressure-variable volume system described elsewhere[36]. The membranes were placed into the permeation cell with an effective permeation area of 12.5 cm^2 and exposed to pure CH_4 or CO_2 gas. Feed pressure was 4 bar gauge and the temperature was 27°C. Pressure-normalized flux (permeance) of gas *i* was calculated as follows:

$$(\frac{P_i}{l}) = \frac{1}{A\Delta p} \times \frac{dV_i}{dt} \quad (1)$$

where *i* represents the gas penetrant, V_i is the volume of gas permeated through the membrane (cm^3, STP), *A* the effective membrane area (cm^2), *t* the permeation time (s) and Δp is the transmembrane pressure drop (cmHg). Permeance is expressed in gas permeation units, GPU, as

1 GPU=1×10^{-6} cm^3 (STP) cm^{-2} s^{-1} $cmHg^{-1}$.

Selectivity was obtained using Eq. (2):

$$\alpha_{i/j} = \frac{(P_i/l)}{(P_j/l)} \quad (2)$$

where $\alpha_{i/j}$ is the selectivity of gas penetrant *i* over gas penetrant *j*, P_i/l and P_j/l are the permeance of gas penetrant *i* and *j*, respectively.

3.0 Result and discussion

3.1 Characterization of virgin and modified ZIF-8

The crystallinity of the prepared ZIF-8 was identified via XRD (**Fig. 1a**). The presence of strong peaks implies high crystallinity of prepared ZIF-8 showing good agreement with previous experimental work[37] and simulated pattern[20]; where the peaks at 2θ = 7.30, 10.35, 12.70, 14.80, 16.40 and 18.00° correspond to planes (110), (200), (211), (220), (310), and (222), respectively. **Fig. 1b** represents the TEM images of the ZIF-8. The prepared ZIF-8 possesses rhombic dodecahedron morphology; showing good agreement with the literature[37]. The particle size of prepared samples was estimated from a series of TEM images to be around 133 nm.

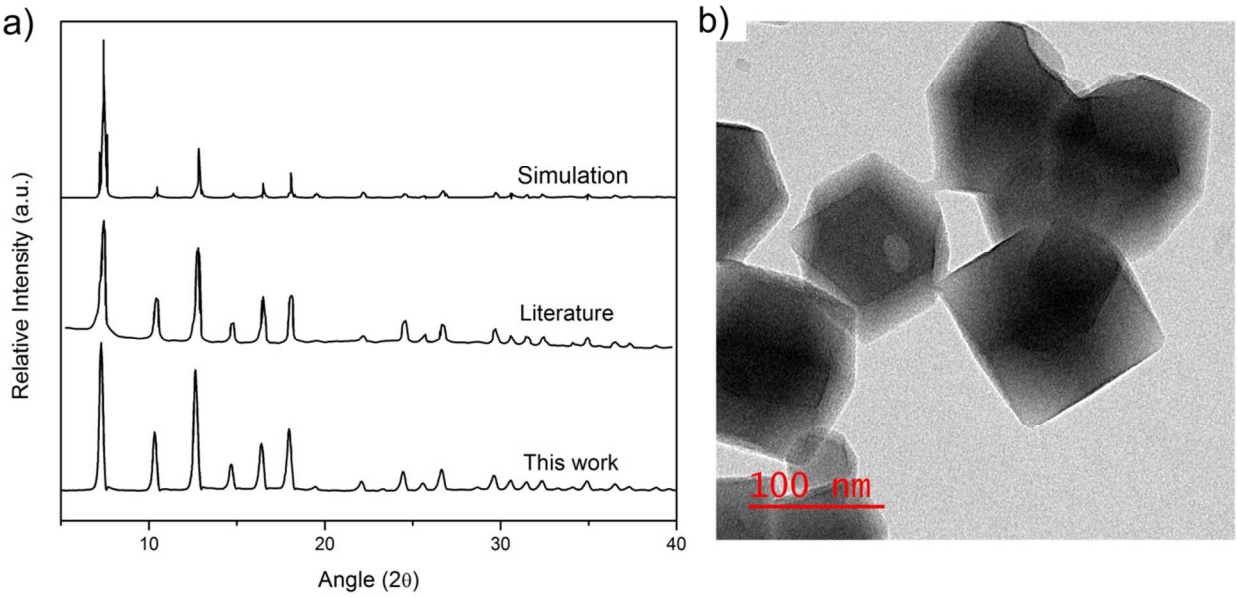

Fig. 1 a) XRD pattern of virgin ZIF-8 as compared with literature[37] and simulated pattern[20], and b) morphology of prepared ZIF-8

The XRD patterns of ZIF-8s after modification are presented in **Fig. 2**. The patterns remains unchanged after modification, indicating strong resistance towards alkaline solution regardless of modification protocols[20, 34]. In the previous report on amine modification it was demonstrated that XRD peak intensity decreased after modification presumably due to impregnation of amine within the ZIF-8 pores causing destructive interference with the XRD peaks[38]. However, TGA analysis (see **Fig. S1**, ESI†) reveals that no weight loss occurred at below 150°C for virgin and modified ZIF-8, indicates ammonium hydroxide solution does not

impregnated within the pores. Moreover, XRD peaks were intensified after modification in this study, further implies that ammonium hydroxide not only was absent within the ZIF-8 pores, but also caused removal of guest molecules. It was also observed that there were no apparent different between the peak width of the virgin and modified ZIF-8. It can postulate that the modification does not provide any significant changes in particle size of ZIF-8. New reflection was also observed at $2\theta = 10.96°$ in all modified samples presumably due to cage reordering on ZIF-8 structure[39].

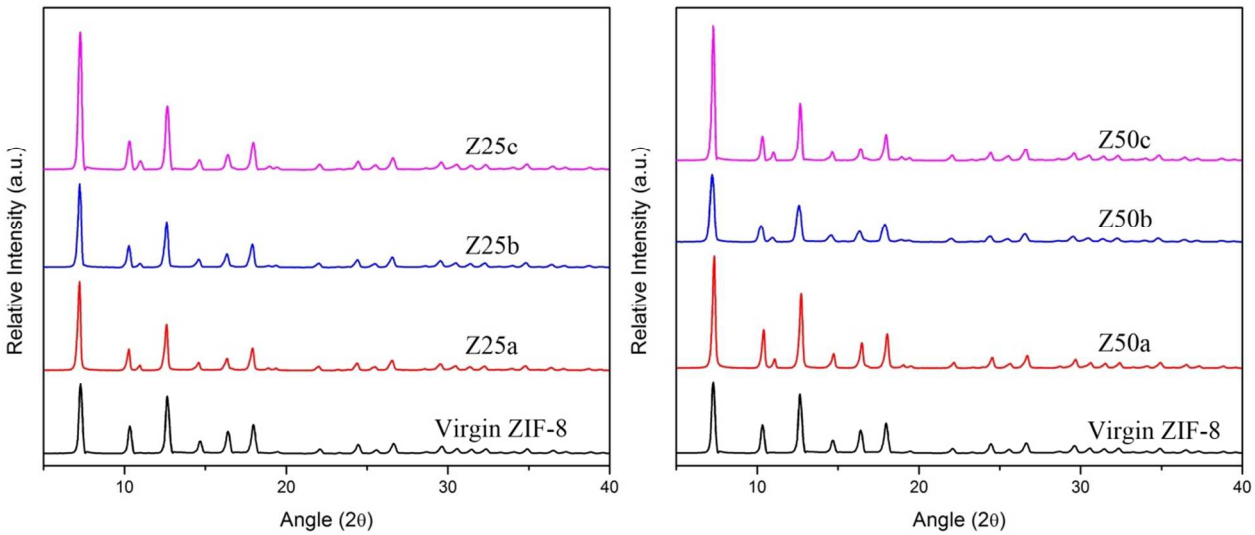

Fig. 2 X-ray diffraction of modified ZIF-8s

N_2 adsorption analysis of prepared ZIF-8s are presented in **Table 2**. The BET surface area of pure ZIF-8 prepared was comparable with the literature values[40, 41]. Increase in BET surface area of modified ZIF-8, except for Z50b and Z50c, is understandable since removal of guest molecules has increased pores availability as observed by intensification in XRD peaks after modifications. It was also observed that the total pore volume of ZIF-8 increased significantly, again except for Z50b and Z50c, after the modification, indicating pore reopening[42] and/or formation of new pores due to cage reordering[39].

The types of pore formed/reopened during the modification were highly dependent on the modification temperature. At ice bath temperature, the availability of mesopores increased dramatically while the micropore accessibility was slightly decreased. As modification temperature increased, the decrease in mesopores is significant probably due to pore constriction

or change of mesopores to micropores (see **Fig. S2-S4**, ESI†). It was also observed that the amount of ammonia solution used for modification plays an important role on surface properties of ZIF-8. Introducing 25mL ammonia solution into ZIF-8 has prompted higher micropore volume whilst constriction of mesopores was less, than 50mL ammonia solution. This behavior presumably caused by dilution of ammonium hydroxide solution with 10mL of deionized water; where more diluted solution ease the dissolution of guest molecules to evacuate the pores and ease modifications to occur. Hence, the total pore volume increased when a smaller amount of ammonia solution was added, with exception of Z25c and Z50c due to pore constriction induced at higher modification temperature.

Table 2 The pore textural properties of virgin and modified ZIF-8

Sample	BET surface area (m^2/g)	Mesopore volume (cm^3/g)	Micropore volume (cm^3/g)	Total pore volume (cm^3/g)
Z0	1031.7	0.2427	0.2995	0.5422
Z25a	1210.7	0.9877	0.2576	1.2453
Z25b	1223.4	0.3141	0.3842	0.6983
Z25c	1250.5	0.1951	0.3852	0.5803
Z50a	1132.2	0.5559	0.2964	0.8523
Z50b	1019.5	0.2368	0.3113	0.5481
Z50c	966.2	0.4983	0.4805	0.9788

The intensifications of XRD peaks and improved surface properties observed in this work after various modifications are contradicting with the previous report, where amine would reside within the pores to cause destructive interference on XRD beam by the blocked pores[34]. Hence, further characterizations are necessary to confirm the modification by ammonium hydroxide. **Fig. 3a** shows the infrared spectrum of virgin and modified ZIF-8s. Most of the spectra are related to the vibrations of the methylimidazole units and thus can be described based on the origin of the bonds. It was observed that the spectra of the samples are in good agreement with other studies[20, 34]. The absorption bands between 3135 and 2929 cm^{-1} can be attributed to the aromatic and the aliphatic C–H stretch of methylimidazole, respectively. The characteristic peak at 1584 cm^{-1} was due to the C=N stretching mode, whereas bands between 1350–1500 cm^{-1} can

be assigned to the entire ring stretching[43]. The peak at 450 cm^{-1} shows the distinct stretching vibration of Zn-N.

There are no apparent differences after ZIF-8 was subjected to different modification protocols due to the presence of similar functional groups also in the virgin ZIF-8. Hence, the IR absorbances on some specific functional groups were more thoroughly studied. The modification of the ZIF-8 has led to the intensification of the IR absorbance peaks coming from C–N stretch (**Fig. 3b**), N–H bend (**Fig. 3c**), and N–H stretch (**Fig. 3d**), thus suggesting that ammonia modification sunder various procedures were successful. It is also observed that the peak intensification was more prominent in Z50-series compared to Z25-series which presumably related to higher ammonium hydroxide content that provide more interaction with ZIF-8 particles.

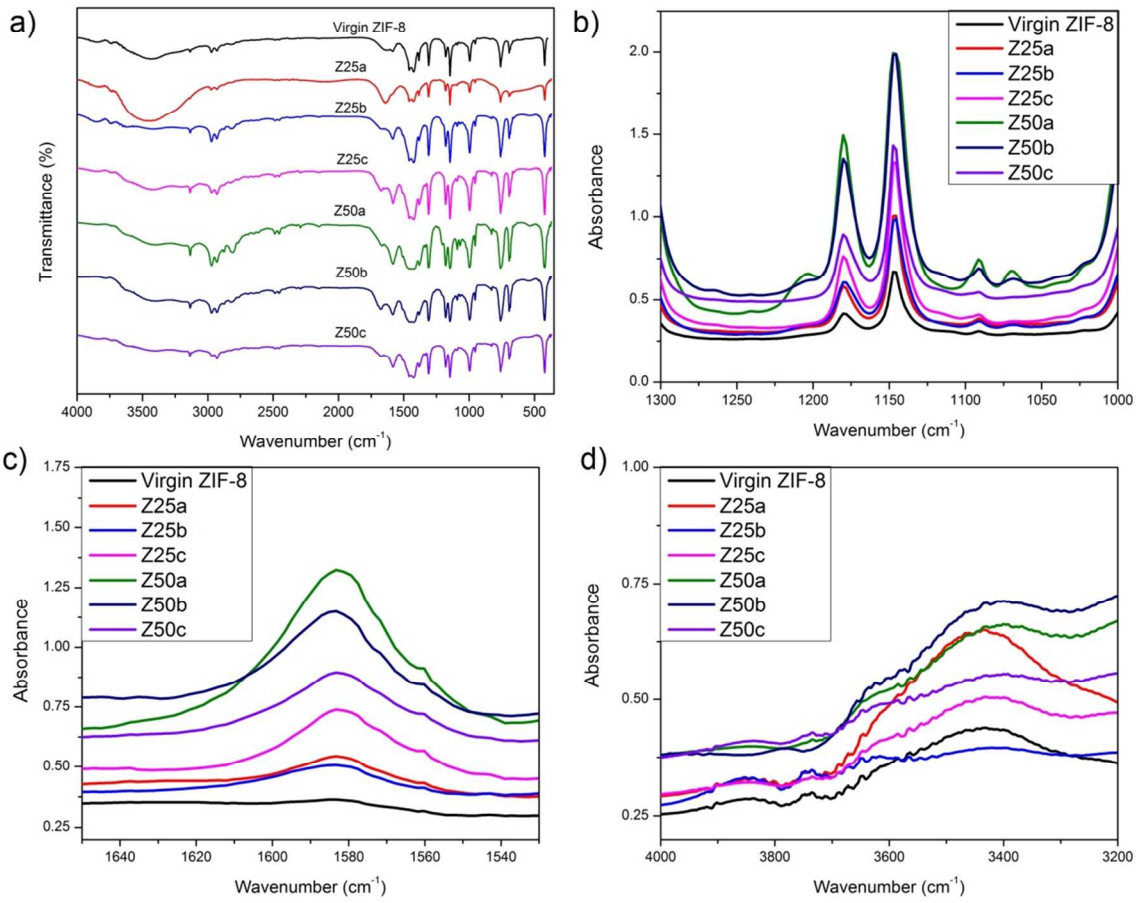

Fig. 3 FTIR analysis of virgin and modified ZIF-8 with a) overall spectrum, and spectra that represent b) aliphatic C–N stretch (1250-1020cm^{-1}), c) N–H bend (1650-1580cm^{-1}), and d) N–H stretch (3400-3250cm^{-1})

The characterizations data presented that the ZIF-8 was successfully modified without ammonia solution being impregnated inside its pores. Liu *e. al*.[44] simulated that in ideal crystal structure of amine-modified ZIF-8, amino group took place near the C=C bond on the methylimidazole linker (**Fig. 4**) with stable structure. The changes of methylimdazole ligands, which responsible for pore opening of 3.4Å in ZIF-8[45], would significantly influence the textural properties as were observed in N_2 adsorption analysis (see **Table 2**) and XRD pattern (see **Fig.2**). It can be postulate that, during modification, N-H functional group deprotonate the C=C in the imidazole linkers and leads to cage reordering while maintaining its overall structure. However, the simulation demonstrated that surface area and pore volume should decrease as modification occurs which contradicts with this work. This contradiction presumably caused by 1) further removal of guest molecule and pore reopening after modification leads to increasing surface area and pore volume, overwhelming the pore constriction by the new N-H group, and 2) randomized N-H group attachment (combination of H_2N-C=C-NH_2, H-C=C-NH_2 and/or none in one crystal unit) experienced by this work, whereas the simulation were based on the idealized structure of amine-modified ZIF-8. Nevertheless, this work shows that amine-group can be introduced through straightforward approach.

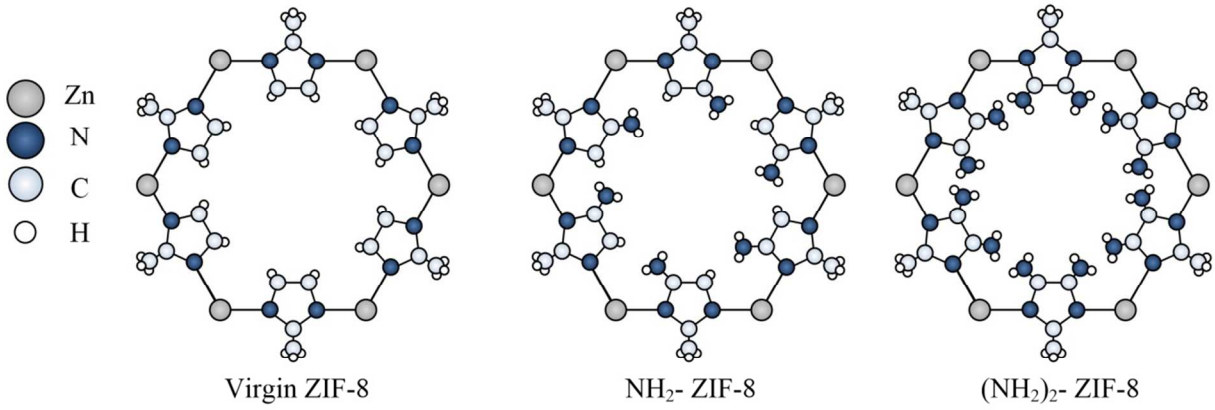

Fig. 4 Idealized crystal structure of amine-modified ZIF-8 (adapted from Liu *et al*.[44]). The NH_2-ZIF-8 represent the $–NH_2$ attached on single side of C=C, while $(NH_2)_2$-ZIF-8 represent the $–NH_2$ group attached on both side of C=C in imidazole linkers.

3.2 MMM characterization

The morphology of prepared membranes is presented in **Fig. 5**. The cross-sectional image of the neat PSf membrane shows an asymmetric structure, with an apparent active layer accompanied by a sponge-like substructure (**Fig. 5a**). The dry phase inversion was introduced to form a thin-selective layer through evaporation of volatile solvent (THF). The sponge-like substructure was also observed as a result of the solvent exchange between NMP and water during the wet inversion.

Similar cross-sectional morphology was observed for all prepared MMMs (see **Fig. 5b** and **Fig. S5, S6**, ESI†) since small amount of fillers were incorporated and similar preparation protocol was used for fabrication. It should be noted that nanoparticles tend to form a bigger cluster due to interaction between their surfaces, especially when a large number of the particles are incorporated. However, no apparent ZIF-8 particles were observed within the membrane cross sectional morphology regardless of modification procedure. In addition, no changes in membrane functional groups as observed via IR analysis (see **Fig. S7**, ESI†) after filler (virgin and modified ZIF-8) incorporation. The results suggested 1) that sonication introduced to the dope preparation was able to break the particle cluster; 2) small amount of ZIF-8 was enough to make significant changes in membrane morphology and functional group; and 3) uniform distribution of the ZIF-8 particles throughout polymer matrix was possible.

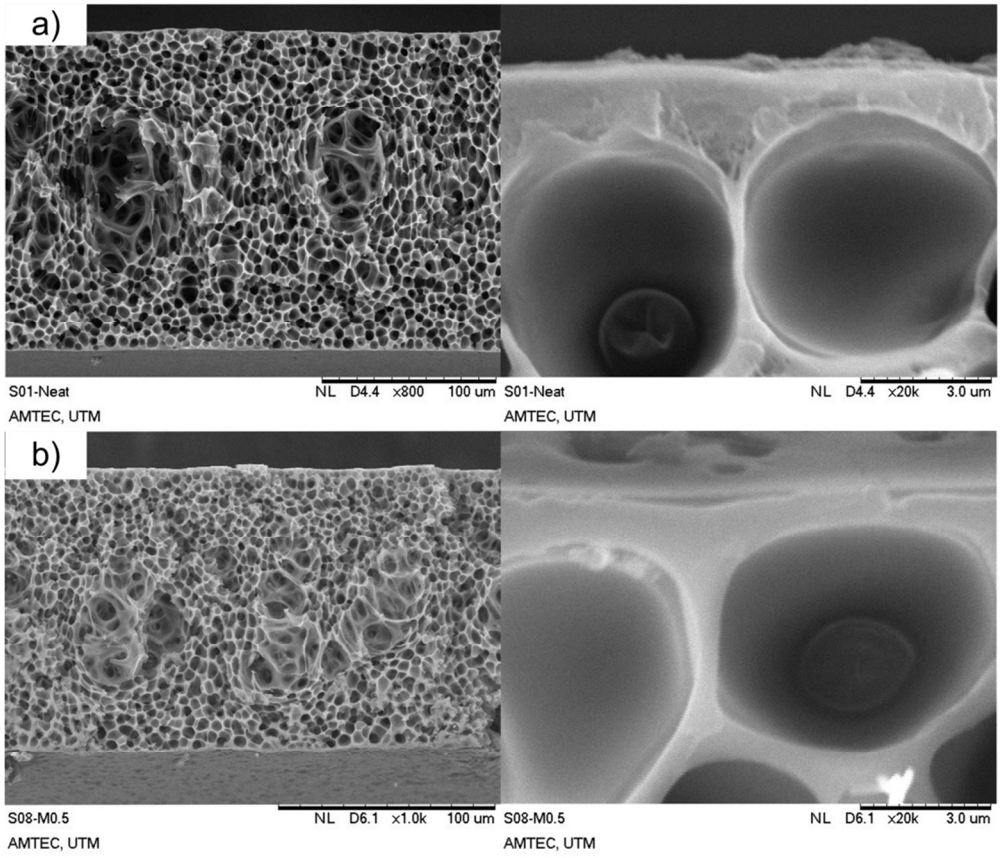

Fig. 5 Cross-sectional membrane morphology of a) neat PSf, and b) M0

The thermal stability of prepared membranes was investigated (see **Fig S8**, ESI†) and no significant difference between thermal stability of pristine PSf and MMMs was observed, which suggested that low ZIF-8 loading did not affect overall thermal stability of prepared membranes. The T_g values of the prepared membranes are summarized in **Table 3**. The T_g of the neat PSf membrane is comparable to the value previously reported[46], indicating high rigidity of the materials. Incorporation of virgin and modified ZIF-8s into PSf matrix provided notable changes in membrane's T_g. The membrane's T_g decreased after virgin ZIF-8 was embedded, indicating increased segmental mobility as the particles reside among the polymer chains. Incorporating modified ZIF-8s into the PSf matrix showed further decrease in membrane's T_g. Hence, it can be postulated that better dispersion of modified ZIF-8s was enabled compared to virgin ZIF-8.

Table 3 Glass transitional temperature of prepared membranes

Sample	Glass transitional temperature (T_g)
Neat PSf	185
M0	175
M25a	165
M25b	156
M25c	160
M50a	151
M50b	146
M50c	167

3.3 Gas Permeation

3.3.1 Influence of virgin and modified ZIF-8s on membrane performance

Table 4 shows the CO_2 permeance and CO_2/CH_4 selectivity of neat PSf membrane and MMMs. The CO_2 permeance and CO_2/CH_4 selectivity of neat PSf are 21.3 ± 6.4 GPU and 19.8, respectively, both lower than the previously reported values due to difference in materials and fabrication history[36, 47, 48]. Upon incorporation of 0.5 wt% (total solids) virgin ZIF-8 (M0), CO_2 permeance and selectivity increased to 29.2 GPU and 23.16, respectively. These phenomena are expected since the open metal sites in ZIF-8 pores have good interaction between quadrupole moment of CO_2, while none with CH_4[49]. Besides, ZIF-8 possesses pore opening of 3.4Å, which introduces molecular sieving as a separation mechanism allowing CO_2 to migrate easily while hindering CH_4 permeation (kinetic diameter of CO_2 is 3.3Å while CH_4 is 3.8Å)[50]. Consequently, significant increase in CO_2/CH_4 selectivity was observed even when ZIF-8 loading was low.

Table 4: The results of membrane permeation studies with neat PSf membrane, MMM with unmodified ZIF-8 and MMMs with modified ZIF-8

Sample	Permeance (GPU) [a]				Ideal CO_2/CH_4 selectivity [b]
	CO_2	±	CH_4	±	
Neat	21.27	6.35	1.08	1.33	19.83
M0	29.19	3.68	1.26	0.05	23.16
M25a	27.05	5.99	1.18	0.18	22.66
M25b	21.21	1.26	0.73	0.01	29.04
M25c	21.16	4.84	0.62	0.228	34.09
M50a	28.19	7.87	1.26	0.35	22.61
M50b	21.74	4.94	1.02	0.39	22.72
M50c	22.41	6.77	0.77	0.17	28.66

[a] GPU = 1 x 10^{-6} cm^3 cm^{-2} s^{-1} $cmHg^{-1}$

[b] Ideal selectivity is based on average of CO_2 and CH_4 permeance

± Represents the standard deviation

The data are reproduced in **Fig. 6** for better interpretation of the effect of the temperature on ZIF-8 modification. The figure shows that, regardless of the modification temperature, all the modified ZIF-8 containing MMMs show CO_2 permeance lower than the virgin ZIF-8 containing MMM (M0) despite the enhancement of BET surface area and total pore volume after modifications, as observed by adsorption experiments. This decrease in the membrane permeance is not due to polymer chain rigidification, since T_g of the MMM decreased when modified ZIF-8 was incorporated. Plausible explanations are 1) CO_2 entrapment within the filler due to through stronger quadrupole-π electron interaction on the N-H group of modified ZIF-8[34, 44] and hindered its diffusion; and 2) decrease in mesopores contribution to the permeation path.

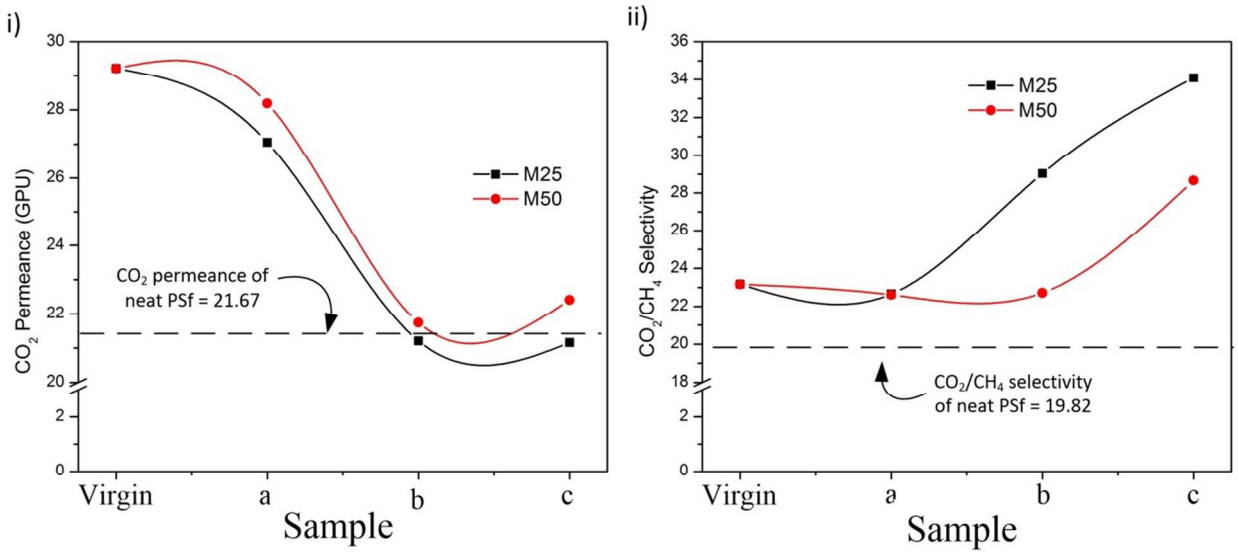

Fig. 6 Gas separation performance of the prepared membranes with i) CO_2 permeance and ii) ideal CO_2/CH_4 selectivity. The MMM containing virgin ZIF-8 is compared with modified ZIF-8 under a) ice bath, b) room temperature, and c) 60°C.

Regarding M25 series, CO_2 permeance decreases progressively from virgin (M0) to ammonium modification at 4°C (M25a) to 27°C (M25b) and to 60°C (M25c). It is recalled that the mesopore volume also decreased progressively from 0.9877 cm^3/g of M25a to 0.1951 cm^3/g of M25c (see **Table 2**), while micropores volume increased from 0.2576 cm^3/g of M25a to 0.3852 cm^3/g of M25c. Therefore, the decrease of CO_2 permeance from M25a to M25c is likely due to the decreased contribution of mesopores and increased contribution of micropores to the gas transport channel.

The decrease in CH_4 permeance from M25a to M25c seems more severe than the decrease of CO_2, since CO_2/CH_4 selectivity keeps increasing from M25a to M25c. This also is due to the increase in the micropores contribution from M25a to M25c. Considering the kinetic diameters of CO_2 (3.3Å) and CH_4 (3.8Å), and the size of the micropores that are likely originating from the 6-ring window aperture of 3.4Å [20], it is obvious that CH_4 transport through the micropores is prohibited while that for CO_2 is allowed. Hence, an increase in micropores contribution leads to an increase in selectivity. The same trend is observed for M50 series. However, unlike M25 series, the selectivity does not change from M50a to M50b but increases significantly from M50b to M50c. This trend parallels to the trend in the micropores volume M-

50a (0.2964 cm^3/g) ≈ M50b (0.3113 cm^3/g) < M50c (0.4805 cm^3/g). Therefore, suppression of CH_4 transport by micropores becomes the most effective for M50c.

Hence, the latter two effects, enhanced interaction between CO_2 and CH_4 hindering effect on modified ZIF-8, have contributed to the significant increase up to 72% in ideal CO_2/CH_4 selectivity compared to neat PSf membrane.

3.3.2 Influence of filler loading

Attempt to further improve the gas separation and permeation performance was implemented by increasing the filler loading. Z25c was chosen for the filler, since M25c demonstrated promising performance with higher selectivity and practically unchanged CO_2 permeance as compared to neat PSf membrane (see **Table 3** and **Fig. 6**).

Quite disappointingly, both CO_2 permeance and selectivity decreased as Z25c loading was increased from 0.5 wt% to 2.0 wt% as shown in **Fig. 7**. This is due to the increase in tortuosity of the permeation path in the presence of a large number of filler particles, which increases the mass transport resistance. In addition, severe Z25c agglomeration might that take place at higher loading has limited the penetrant's access the ZIF-8 pores[50] and dwindle its selective features. Consequently, simultaneous decreased in both CO_2 permeance and ideal CO_2/CH_4 selectivity was observed at higher Z25c loading. Hence, only 0.5wt% (total solids) of Z25c is necessary to improve the membrane selectivity.

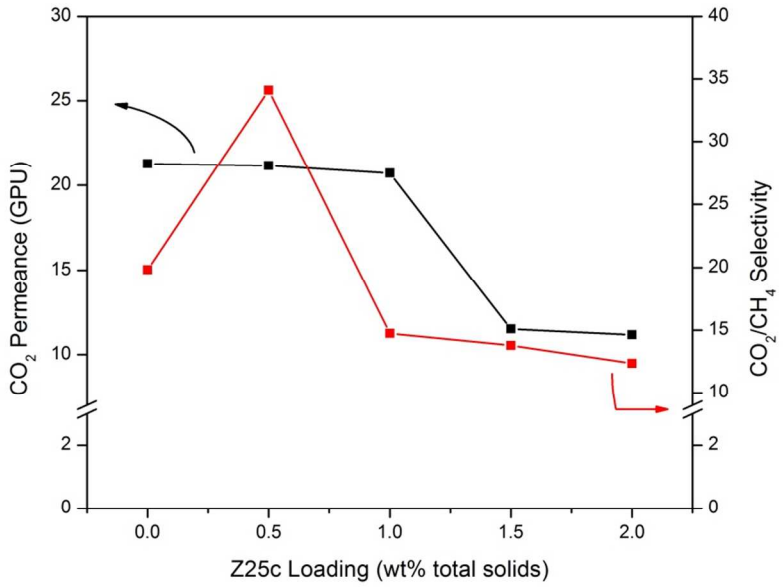

Fig. 7 Separation performance of PSf/Z25c at different filler loadings

3.4 Comparison with literatures

MMMs in which ZIF-8 was incorporated in different polymers have been reported during the past years. Most of polymer/ZIF-8 MMMs were prepared as dense membranes in earlier studies focusing on the changes in gas solubility and diffusivity with ZIF-8 incorporation and CO_2 permeability was reported in Barrer. Whereas, asymmetric membranes were prepared in this study since it is more relevant to practical applications and CO_2 permeance is reported in GPU. To enable the performance comparison with other ZIF-8 incorporated MMMs, the selective layer thickness of the neat PSf and M25c was evaluated from the FESEM images, as shown in **Fig. 8**. The selective layer thickness for PSf and M25c were estimated around 0.238 and 0.341 μm, respectively, and the CO_2 permeabilities were calculated to be 5.06 and 7.26 Barrer, respectively.

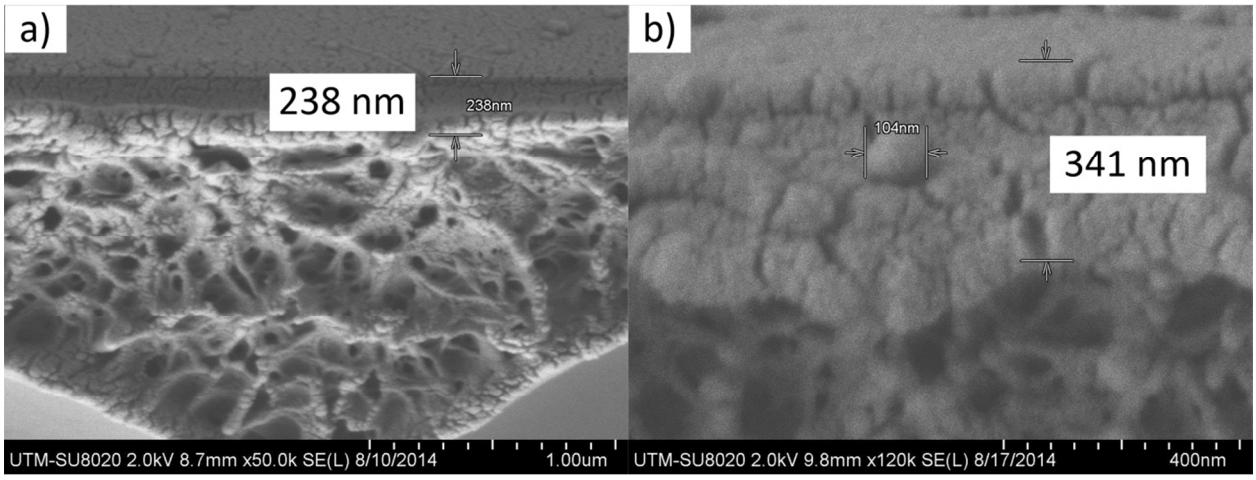

Fig. 8 Skin layer thickness of a) neat PSf membrane, and b) M25c

The intrinsic CO_2 permeability and CO_2/CH_4 electivity of PSf are reported to be 4.4 Barrer and 30.0, respectively[51]. Compared to the reported values, the selectivity obtained in this study (19.8) is significantly lower and compensated by higher CO_2 permeability (5.06 Barrer). The performances of various polymer/ZIF-8 MMMs reported in the literature are tabulated in **Table 5** and compared with M25c of this study. Most notable is the work by Ordoñez *et al*.[50] where 50wt% (total solids) of ZIF-8 was incorporated in Matrimid®. They achieved CO_2/CH_4 selectivity of 124.89, which is 187% better than the neat Matrimid® membrane. This level of high ZIF-8 loading is typical of dense MMMs without suffering from defective polymer-filler interface and the dispersed ZIF-8 can be fully utilized to facilitate the separation performance. For this reason, the dense MMMs could surpass the Robeson upper bound limit.

In contrast, the fabrication of asymmetric membrane does not allow high ZIF-8 loading. In this study, the loading of modified ZIF-8 was as low as 0.5 wt%, which significantly limited the potential capacity of ZIF-8 filler[50, 52-54]. Thus, the MMM fabricated in this study does not stand out among the available data of ZIF-8 MMMs. Nevertheless, the performance of M25c membrane is considered a remarkable improvement from the neat PSf membrane. The ammonia modification has improved surface area and micropores volume of ZIF-8 with the presence of N-H functional group. The resulted MMM is more CO_2 permeable (7.26 Barrer) and CO_2-selective (34.09), superior than neat PSf membrane despite its limited filler loading (0.5wt%). These improvement are in well agreement with simulation[44] and experimental[34, 42] works on CO_2 adsorption in amine-modified ZIF-8. Hence, straightforward modification through ammonium

solution on ZIF-8 proposed in this work would motivate towards future development of MOF-based MMMs for CO_2 removal.

Table 5 Comparison between virgin ZIF-8-based MMM and this work

Polymer	Membrane Configuration	Loading (wt% total solids)	% changes in CO_2 permeability	% changes in CO_2/CH_4 selectivity	Reference
Matrimid	Dense	50	-54%	187%	[50]
PPEES	Dense	10	39%	29%	[52]
Matrimid	Dense	30	219%	15%	[17]
Matrimid	Dense	5	25%	11%	[55]
PIM-1	Dense	28[v]	-3%	31%	[53]
PMPS	Dense	8.3	171%	-12%	[54]
PSf	Asymmetric	0.5	43%	72%	This work

[v] volumetric percent

4.0 Conclusion

ZIF-8s which underwent ammonia modification under various conditions exhibited significant changes in its properties, i.e. phase crystallinity, pore properties and BET surface area increased, while preserving its overall structure. The MMM with modified ZIF-8 has shown substantial increased in ideal CO_2/CH_4 selectivity, especially for ZIF-8 modified under 25mL ammonium hydroxide solution at 60°C. Formation of new micropores while disappearances of mesopores have hindered CH_4 permeation across the membrane, combined with the introductory of N-H functional group within the ZIF-8 after modification resulting in significant improvement in 43% of CO_2 permeability and 72% of ideal CO_2/CH_4 selectivity by only minimal loading (0.5wt%). Increased the filler loading did not necessarily improve the MMM performances in CO_2/CH_4 separation due to particle agglomeration that restricts penetrant access to the pores. Hence, the ammonia modification proposed in this study has proven as a straightforward approaches to simultaneously increased CO_2 permeability and ideal CO_2/CH_4 selectivity, would beneficial for future works focused on gas separation MMM, especially for CO_2 separation.

Acknowledgement

The authors gratefully acknowledge the Ministry of Education (MOE) for the scholarship and Long-Term Research Grant Scheme (LRGS) Program under Universiti Teknologi Malaysia with the grant number Q.J130000.2452.04H71.

References

1. Tom Cnop, David Dortmundt and M. Schott, *UOP Continued Development of Gas Separation Membranes Tech Paper*, 2007.
2. M. Mofarahi, Y. Khojasteh, H. Khaledi and A. Farahnak, *Energy*, 2008, 33, 1311-1319.
3. M. Wang, A. Lawal, P. Stephenson, J. Sidders and C. Ramshaw, *Chemical Engineering Research and Design*, 2011, 89, 1609-1624.
4. T. E. Rufford, S. Smart, G. C. Y. Watson, B. F. Graham, J. Boxall, J. C. Diniz da Costa and E. F. May, *Journal of Petroleum Science and Engineering*, 2012, 94–95, 123-154.
5. R. W. Baker, in *Membrane Technology and Applications*, John Wiley & Sons, Ltd, 2012, pp. 325-378.
6. R. W. Baker and B. T. Low, *Macromolecules*, 2014, 47, 6999-7013.
7. L. M. Robeson, *Journal of Membrane Science*, 2008, 320, 390-400.
8. P. M. Budd and N. B. McKeown, *Polymer Chemistry*, 2010, 1, 63-68.
9. S. Kim, L. Chen, J. K. Johnson and E. Marand, *Journal of Membrane Science*, 2007, 294, 147-158.
10. R. T. Adams, J. S. Lee, T.-H. Bae, J. K. Ward, J. R. Johnson, C. W. Jones, S. Nair and W. J. Koros, *Journal of Membrane Science*, 2011, 367, 197-203.
11. K. Díaz, L. Garrido, M. López-González, L. F. del Castillo and E. Riande, *Macromolecules*, 2010, 43, 316-325.
12. Y. Yampolskii, *Macromolecules*, 2012, 45, 3298-3311.
13. C. Casado-Coterillo, J. Soto, M. T. Jimaré, S. Valencia, A. Corma, C. Téllez and J. Coronas, *Chemical Engineering Science*, 2012, 73, 116-122.
14. A. F. Ismail, N. H. Rahim, A. Mustafa, T. Matsuura, B. C. Ng, S. Abdullah and S. A. Hashemifard, *Separation and Purification Technology*, 2011, 80, 20-31.
15. D. Q. Vu, W. J. Koros and S. J. Miller, *Journal of Membrane Science*, 2003, 221, 233-239.
16. M. Anson, J. Marchese, E. Garis, N. Ochoa and C. Pagliero, *Journal of Membrane Science*, 2004, 243, 19-28.
17. S. Basu, A. Cano-Odena and I. F. J. Vankelecom, *Separation and Purification Technology*, 2011, 81, 31-40.
18. M. A. Aroon, A. F. Ismail, T. Matsuura and M. M. Montazer-Rahmati, *Separation and Purification Technology*, 2010, 75, 229-242.
19. J. Yao and H. Wang, *Chemical Society reviews*, 2014, 43, 4470-4493.
20. K. S. Park, Z. Ni, A. P. Cote, J. Y. Choi, R. Huang, F. J. Uribe-Romo, H. K. Chae, M. O'Keeffe and O. M. Yaghi, *Proceedings of the National Academy of Sciences of the United States of America*, 2006, 103, 10186-10191.
21. S. A. Moggach, T. D. Bennett and A. K. Cheetham, *Angewandte Chemie*, 2009, 48, 7087-7089.
22. J. C. Tan, T. D. Bennett and A. K. Cheetham, *Proceedings of the National Academy of Sciences*, 2010, 107, 9938-9943.
23. Y.-S. Bae, O. K. Farha, J. T. Hupp and R. Q. Snurr, *Journal of Materials Chemistry*, 2009, 19, 2131.
24. Y.-S. Bae, B. G. Hauser, O. K. Farha, J. T. Hupp and R. Q. Snurr, *Microporous and Mesoporous Materials*, 2011, 141, 231-235.

25. S. R. Caskey, A. G. Wong-Foy and A. J. Matzger, *Journal of the American Chemical Society*, 2008, 130, 10870-10871.
26. Z. Y. Yeo, S.-P. Chai, P. W. Zhu and A. R. Mohamed, *Microporous and Mesoporous Materials*, 2014, 196, 79-88.
27. W. N. W. Salleh and A. F. Ismail, *Separation and Purification Technology*, 2011, 80, 541-548.
28. J.-R. Li, Y. Ma, M. C. McCarthy, J. Sculley, J. Yu, H.-K. Jeong, P. B. Balbuena and H.-C. Zhou, *Coordination Chemistry Reviews*, 2011, 255, 1791-1823.
29. F.-J. Ma, S.-X. Liu, D.-D. Liang, G.-J. Ren, F. Wei, Y.-G. Chen and Z.-M. Su, *Journal of Solid State Chemistry*, 2011, 184, 3034-3039.
30. Q.-L. Zhu and Q. Xu, *Chemical Society reviews*, 2014, 43, 5468-5512.
31. Z. Wang and S. M. Cohen, *Chemical Society reviews*, 2009, 38, 1315-1329.
32. K. L. Mulfort and J. T. Hupp, *Inorganic chemistry*, 2008, 47, 7936-7938.
33. S. Choi, T. Watanabe, T.-H. Bae, D. S. Sholl and C. W. Jones, *The Journal of Physical Chemistry Letters*, 2012, 3, 1136-1141.
34. Z. Zhang, S. Xian, H. Xi, H. Wang and Z. Li, *Chemical Engineering Science*, 2011, 66, 4878-4888.
35. N. A. H. M. Nordin, A. F. Ismail, A. Mustafa, P. S. Goh, D. Rana and T. Matsuura, *RSC Advances*, 2014, 4, 33292-33300.
36. A. F. Ismail and P. Y. Lai, *Separation and Purification Technology*, 2003, 33, 127-143.
37. A. F. Gross, E. Sherman and J. J. Vajo, *Dalton transactions*, 2012, 41, 5458.
38. B. Arstad, H. Fjellvåg, K. Kongshaug, O. Swang and R. Blom, *Adsorption*, 2008, 14, 755-762.
39. F. Schröder, D. Esken, M. Cokoja, M. W. E. van den Berg, O. I. Lebedev, G. Van Tendeloo, B. Walaszek, G. Buntkowsky, H.-H. Limbach, B. Chaudret and R. A. Fischer, *Journal of the American Chemical Society*, 2008, 130, 6119-6130.
40. Y. Pan, Y. Liu, G. Zeng, L. Zhao and Z. Lai, *Chemical communications*, 2011, 47, 2071-2073.
41. J. Cravillon, S. Münzer, S.-J. Lohmeier, A. Feldhoff, K. Huber and M. Wiebcke, *Chemistry of Materials*, 2009, 21, 1410-1412.
42. Z. Zhang, S. Xian, Q. Xia, H. Wang, Z. Li and J. Li, *AIChE Journal*, 2013, 59, 2195-2206.
43. Y. Hu, H. Kazemian, S. Rohani, Y. Huang and Y. Song, *Chemical communications*, 2011, 47, 12694-12696.
44. D. Liu, Y. Wu, Q. Xia, Z. Li and H. Xi, *Adsorption*, 2013, 19, 25-37.
45. L. Hertäg, H. Bux, J. Caro, C. Chmelik, T. Remsungnen, M. Knauth and S. Fritzsche, *Journal of Membrane Science*, 2011, 377, 36-41.
46. G. C. Kapantaidakis, S. P. Kaldis, X. S. Dabou and G. P. Sakellaropoulos, *Journal of Membrane Science*, 1996, 110, 239-247.
47. B. Zornoza, A. Martinez-Joaristi, P. Serra-Crespo, C. Tellez, J. Coronas, J. Gascon and F. Kapteijn, *Chemical communications*, 2011, 47, 9522-9524.
48. A. F. Ismail and W. Lorna, *Separation and Purification Technology*, 2003, 30, 37-46.
49. R. Banerjee, H. Furukawa, D. Britt, C. Knobler, M. O'Keeffe and O. M. Yaghi, *Journal of the American Chemical Society*, 2009, 131, 3875-3877.
50. M. J. C. Ordoñez, K. J. Balkus, J. P. Ferraris and I. H. Musselman, *Journal of Membrane Science*, 2010, 361, 28-37.

51. M. Mulder, *Basic Principles of Membrane Technology*, Kluwer Academic Publisher, Netherlands, 2nd edn., 1996.
52. K. Díaz, M. López-González, L. F. del Castillo and E. Riande, *Journal of Membrane Science*, 2011, 383, 206-213.
53. A. F. Bushell, M. P. Attfield, C. R. Mason, P. M. Budd, Y. Yampolskii, L. Starannikova, A. Rebrov, F. Bazzarelli, P. Bernardo, J. Carolus Jansen, M. Lanč, K. Friess, V. Shantarovich, V. Gustov and V. Isaeva, *Journal of Membrane Science*, 2013, 427, 48-62.
54. L. Diestel, X. L. Liu, Y. S. Li, W. S. Yang and J. Caro, *Microporous and Mesoporous Materials*, 2014, 189, 210-215.
55. Q. Song, S. K. Nataraj, M. V. Roussenova, J. C. Tan, D. J. Hughes, W. Li, P. Bourgoin, M. A. Alam, A. K. Cheetham, S. A. Al-Muhtaseb and E. Sivaniah, *Energy & Environmental Science*, 2012, 5, 8359-8369.